

UC Irvine

UC Irvine Previously Published Works

Title

Accumulation-mode aerosol number concentrations in the Arctic during the ARCTAS aircraft campaign: Long-range transport of polluted and clean air from the Asian continent

Permalink

<https://escholarship.org/uc/item/5216p0pn>

Journal

Journal of Geophysical Research Atmospheres, 116(20)

ISSN

0148-0227

Authors

Matsui, H
Kondo, Y
Moteki, N
[et al.](#)

Publication Date

2011

DOI

10.1029/2011JD016189

Copyright Information

This work is made available under the terms of a Creative Commons Attribution License, available at <https://creativecommons.org/licenses/by/4.0/>

Peer reviewed

Accumulation-mode aerosol number concentrations in the Arctic during the ARCTAS aircraft campaign: Long-range transport of polluted and clean air from the Asian continent

H. Matsui,¹ Y. Kondo,¹ N. Moteki,¹ N. Takegawa,² L. K. Sahu,³ M. Koike,¹ Y. Zhao,⁴ H. E. Fuelberg,⁵ W. R. Sessions,⁵ G. Diskin,⁶ B. E. Anderson,⁶ D. R. Blake,⁷ A. Wisthaler,⁸ M. J. Cubison,⁹ and J. L. Jimenez⁹

Received 2 May 2011; revised 9 August 2011; accepted 9 August 2011; published 29 October 2011.

[1] We evaluate the impact of transport from midlatitudes on aerosol number concentrations in the accumulation mode (light-scattering particles (LSP) with diameters >180 nm) in the Arctic during the Arctic Research of the Composition of the Troposphere from Aircraft and Satellites (ARCTAS) campaign. We focus on transport from the Asian continent. We find marked contrasts in the number concentration (N_{LSP}), transport efficiency ($TE_{N_{LSP}}$, the fraction transported from sources to the Arctic), size distribution, and the chemical composition of aerosols between air parcels from anthropogenic sources in East Asia (Asian AN) and biomass burning sources in Russia and Kazakhstan (Russian BB). Asian AN air had lower N_{LSP} and $TE_{N_{LSP}}$ (25 cm^{-3} and 18% in spring and 6.2 cm^{-3} and 3.0% in summer) than Russian BB air (280 cm^{-3} and 97% in spring and 36 cm^{-3} and 7.6% in summer) due to more efficient wet scavenging during transport from East Asia. Russian BB in this spring is the most important source of accumulation-mode aerosols over the Arctic, and BB emissions are found to be the primary source of aerosols within all the data in spring during ARCTAS. On the other hand, the contribution of Asian AN transport had a negligible effect on the accumulation-mode aerosol number concentration in the Arctic during ARCTAS. Compared with background air, N_{LSP} was 2.3–4.7 times greater for Russian BB air but 2.4–2.6 times less for Asian AN air in both spring and summer. This result shows that the transport of Asian AN air decreases aerosol number concentrations in the Arctic, despite the large emissions of aerosols in East Asia. The very low aerosol number concentrations in Asian AN air were caused by wet removal during vertical transport in association with warm conveyor belts (WCBs). Therefore, this cleansing effect will be prominent for air transported via WCBs from other midlatitude regions and seasons. The inflow of clean midlatitude air can potentially have an important impact on accumulation-mode aerosol number concentrations in the Arctic.

Citation: Matsui, H., et al. (2011), Accumulation-mode aerosol number concentrations in the Arctic during the ARCTAS aircraft campaign: Long-range transport of polluted and clean air from the Asian continent, *J. Geophys. Res.*, 116, D20217, doi:10.1029/2011JD016189.

1. Introduction

[2] High concentrations of aerosols occur in the Arctic (Arctic Haze) in winter and spring because of efficient

transport of pollutants from midlatitudes and slow removal processes in these seasons [Barrie, 1986; Shaw, 1995]. These aerosols are considered to significantly contribute to Arctic warming [Shindell and Faluvegi, 2009] through reduction of the surface albedo [Flanner et al., 2007, 2009; Hansen and Nazarenko, 2004] and enhancement of cloud

¹Department of Earth and Planetary Science, Graduate School of Science, University of Tokyo, Tokyo, Japan.

²Research Center for Advanced Science and Technology, University of Tokyo, Tokyo, Japan.

³Department of Space, Physical Research Laboratory, Ahmedabad, India.

⁴Air Quality Research Center, University of California, Davis, California, USA.

⁵Department of Meteorology, Florida State University, Tallahassee, Florida, USA.

⁶Chemistry and Dynamics Branch, NASA Langley Research Center, Hampton, Virginia, USA.

⁷Department of Chemistry, University of California, Irvine, California, USA.

⁸Institute of Ion Physics and Applied Physics, University of Innsbruck, Innsbruck, Austria.

⁹Department of Chemistry and Biochemistry and CIRES, University of Colorado at Boulder, Boulder, Colorado, USA.

Table 1. Acronyms Used in This Study

| Terminology | Definition |
|--|---|
| LSP | Light-scattering particles |
| BC | Black carbon |
| M_{BC} | Mass concentration of BC |
| N_{LSP}, N_{BC} | Number concentration of LSP and BC |
| N_{CPC} | Number concentration measured by CPC (>4 nm) |
| V_{LSP}, V_{BC} | Volume concentration of LSP and BC |
| $TE_{N_{LSP}}, TE_{N_{BC}}, TE_{V_{LSP}}, TE_{V_{BC}}$ | Transport efficiency of N_{LSP} , N_{BC} , V_{LSP} , and V_{BC} defined by equation (1) |
| $F_{N_{LSP}}, F_{N_{BC}}, F_{V_{LSP}}, F_{V_{BC}}$ | Fractional source contribution to the total amount of N_{LSP} , V_{LSP} , N_{BC} , and M_{BC} defined by equation (2) |
| R_{SO_4}, R_{ORG} | Average mass ratio of sulfate and organic aerosols to the total measured mass concentrations |
| Asian AN | Air parcel from anthropogenic sources in East Asia |
| Russian BB | Air parcel from biomass burning sources in Russia and Kazakhstan |
| APT | Accumulated precipitation along individual trajectories |
| WCB | Warm conveyor belt |
| CCN | Cloud condensation nuclei |
| AIE | Aerosol indirect effect |
| BL | Boundary layer |
| LT | Lower troposphere |
| MT | Middle troposphere |
| UT | Upper troposphere |

longwave emissivity [Lubin and Vogelmann, 2006; Garrett and Zhao, 2006].

[3] Previous studies have suggested that Arctic pollution in the lower troposphere (LT) is mainly from northern Eurasia (Europe and Siberia) [e.g., Stohl, 2006; Law and Stohl, 2007; Klonecki et al., 2003; Huang et al., 2010]. However, the sources, transport pathways, removal processes, and distributions of aerosols in the Arctic are still uncertain, particularly in the middle and upper troposphere (MT and UT). Simulated aerosol concentrations in the Arctic are generally quite variable between models, primarily due to the different treatments of transport, transformation, and removal processes in different models [Shindell et al., 2008; Koch et al., 2009]. To reduce these uncertainties, it is essential to validate these model calculations with detailed measurements of aerosols (e.g., number and volume concentrations, chemical composition) and information on sources and transport processes.

[4] A number of studies on aerosol number concentrations have been made in the Arctic previously based on aircraft measurements [e.g., Schnell and Raatz, 1984; Radke et al., 1984; Barrie, 1986; Leaitch et al., 1989, 1994; Brock et al., 1990; Yum and Hudson, 2001; Yamanouchi et al., 2005; Engvall et al., 2008a] and near-surface measurements, e.g., at Barrow station, Alaska, at Alert station, Canada, and at Zeppelin station, Norway [e.g., Barrie, 1986; Staebler et al., 1994, 1999; Quinn et al., 2002; Ström et al., 2003; Heintzenberg et al., 2006; Engvall et al., 2008b]. Some studies have reported vertical profiles of aerosol number concentration in the Arctic including MT and UT, e.g., vertical profiles from near the surface to 5–7 km over the Alaskan Arctic during Arctic Gas and Aerosol Sampling Program (AGASP) campaign in March 1983 [Schnell and Raatz, 1984], over the Canadian Arctic during AGASP II in April 1986 [Leaitch et al., 1989] and during April 1992

[Leaitch et al., 1994], over the Alaskan Arctic Ocean during May 1998 [Yum and Hudson, 2001], and during the Arctic Study of Tropospheric Aerosol and Radiation (ASTAR) campaign in March 2000 [Yamanouchi et al., 2005] and in May–June 2004 [Engvall et al., 2008a]. However, they did not fully clarify the impact of different source regions and types (anthropogenic or biomass burning) of aerosols in the MT and UT and did not interpret aerosol pathways and processes during long-range transport from sources to the Arctic.

[5] Aerosol number concentrations were measured extensively during the NASA Arctic Research of the Composition of the Troposphere from Aircraft and Satellites (ARCTAS) aircraft campaign conducted in and near the Arctic in April and June–July 2008 [Jacob et al., 2010]. Using these data, we evaluate the impacts of transport from the midlatitudes on aerosol number concentrations in the accumulation mode (measured diameters of 180–860 nm (section 2)) in the Arctic, especially from the Asian continent. We focus on air parcels from Asia because the ARCTAS measurements were made mainly over the Alaskan and Canadian Arctic region, which received air mostly originating from Asia [Fuelberg et al., 2010]. We characterize differences in accumulation-mode number concentration, size distribution, chemical composition, and transport efficiency of aerosols between air parcels influenced by anthropogenic emissions in East Asia (Asian AN) (e.g., China, Korea, and Japan) and emissions from biomass burning in Russia and Kazakhstan (Russian BB). Acronyms used in this study are summarized in Table 1.

2. Measurements and Methods

2.1. ARCTAS Observations

[6] Measurements of aerosols and other related species were made on board the NASA DC-8 aircraft during the ARCTAS aircraft campaign. Overviews of the ARCTAS campaign and meteorological conditions during the observation periods have been given by Jacob et al. [2010] and Fuelberg et al. [2010], respectively. In this study, we used North American Arctic data (one-minute average data), which was selected by Matsui et al. [2011] (referred to as M2011, hereafter): 5 flights (Flights 06–10) over the Alaskan Arctic from 8 to 17 April (ARCTAS-A) and 2 flights (Flights 21–22) over the Canadian Arctic from 8 to 9 July (ARCTAS-B) (Figure 1). These data do not contain air parcels in the stratosphere (defined as ozone mixing ratio >120 ppbv) and in clouds (defined as liquid or ice water contents >0.01 g m $^{-3}$) (M2011). M2011 suggested using satellite measurements that these flights during the ARCTAS-A and ARCTAS-B campaigns were representative of the North American Arctic in April and July 2008, respectively.

[7] The number and volume size distributions of light-scattering particles (LSP), which do not contain black carbon (BC) particles with volume-equivalent dry diameters larger than about 180 nm, were measured together with BC-containing particles by a Single Particle Soot Photometer (SP2) with high accuracy and temporal resolution [Moteiki and Kondo, 2007]. We denote the measured number and volume concentrations of LSP at standard temperature and pressure (STP) as N_{LSP} and V_{LSP} , respectively, and number, mass, and volume concentrations of BC at STP as N_{BC} ,

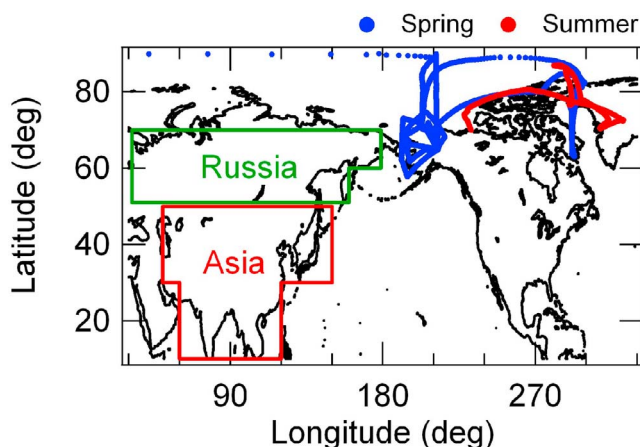


Figure 1. Flight tracks in spring (blue, 5 flights) and summer (red, 2 flights) in and near the Arctic during the ARCTAS campaign used in this study. Green and red squares show the source regions defined in this study.

M_{BC} , and V_{BC} , respectively. Detailed descriptions of the SP2 used during the ARCTAS campaign are given elsewhere [Moteiki and Kondo, 2010; Kondo et al., 2010, 2011]. During ARCTAS, the SP2 covered mass equivalent diameters of 80–860 nm for BC particles and 180–860 nm for LSP [Kondo et al., 2011]. LSP consisted of 89% and 97% of measured aerosol number and volume (LSP + BC), respectively, during the ARCTAS periods (average of 7 flights used in this study). Since the diameter of 180 nm corresponds approximately to the critical diameter of CCN at low supersaturations (supersaturation of about 0.1% and hygroscopicity of about 0.3 [Petters and Kreidenweis, 2007]), N_{LSP} approximates the concentrations of particles that act as CCN at 0.1% supersaturation. We also used the measurements of carbon monoxide (CO) [Sachse et al., 1987], acetonitrile (CH_3CN) [Wisthaler et al., 2002], dichloromethane (CH_2Cl_2) [Blake et al., 2003], the aerosol chemical composition of particulate matter smaller than 1 μm (PM_{10}) [DeCarlo et al., 2006; Dunlea et al., 2009], the total aerosol number concentration (>4 nm) measured by condensation particle counters (N_{CPC}) [Anderson et al., 1998], and aerosol volume concentrations in the coarse mode determined by a TSI Aerodynamic Particle Sizer (APS) Model 3321 (aerodynamic diameter of 0.7–5 μm). Since the lifetimes of CO, CH_3CN , and CH_2Cl_2 are longer than one month in the atmosphere, we represent the short-term variability of these species by the differences between the measured and background concentrations of these species, denoted ΔCO , ΔCH_3CN , and ΔCH_2Cl_2 , respectively. The definitions of the background concentrations are given by M2011.

2.2. Methods of Data Analysis

[8] The methods of data analysis used in this study are similar to those of M2011. In brief, source regions of individual air parcels were estimated from 10-day backward trajectories released along the flight tracks [Fuelberg et al., 2010, and references therein]. The source regions were defined by M2011 as the boundary layer (BL) from the surface to 700 hPa over four regions: Europe, Russia (including Kazakhstan), Asia (including China, Korea, and Japan), and

North America. We focus on source regions of Asia and Russia, shown in Figure 1. In this study, air parcels were classified as Russia, Asia, R+A (trajectories passing over source regions of both Russia and Asia), and other (from Europe or North America or source-unidentified data).

[9] It is a key issue to understand the relative contributions of AN and BB in the Arctic because recent studies suggested the importance of BB emissions to Arctic haze [e.g., Warneke et al., 2009, 2010]. In this study, source types (AN or BB) of individual air parcels were estimated from the concentrations of ΔCH_2Cl_2 and ΔCH_3CN , which have been often used as tracers of AN and BB sources, respectively [e.g., Chen et al., 2007; Warneke et al., 2006]. AN air was defined as having high ΔCH_2Cl_2 (>5 pptv) and low ΔCH_3CN (<100 pptv), while BB air was defined as having high ΔCH_3CN (>50 pptv) and low ΔCH_2Cl_2 (<10 pptv) (Figure 3 of M2011). Air parcels with high ΔCH_2Cl_2 and ΔCH_3CN were influenced by both AN and BB sources, and they are denoted as ANBB. The criteria of source regions and types was chosen so that we examine relatively fresh (within 10 days prior to measurement) air parcels clearly influenced by AN and BB emissions. As a result, the sources (both regions and types) were identified for about 25% of all the data (referred to as source-identified data) (M2011).

[10] We calculated accumulated precipitation along individual trajectories (APT) using Global Precipitation Climatology Project (GPCP) global precipitation data [Huffman et al., 2001; Adler et al., 2003] as in work by M2011. The amount of precipitation was summed (accumulated) along individual trajectories from where the air was sampled to when each trajectory reached one of the source regions (t hours before the measurements, dependent on trajectories) plus an additional 48 h within the sources, because air parcels may have already been influenced by precipitation within the source regions. Thus, the integration period for calculating the APT was $t + 48$ h (<10 days). The rationale for choosing the additional 48 h was discussed by M2011. Results did not change qualitatively when other integration periods ($t + 24$ h or t hours) were used for calculating APT values. We used the APT values as a measure of wet removal processes during transport. We note that APT is a broad measure because we use surface precipitation amounts. Precipitation may occur below air parcels, that does not affect aerosols in the air parcels.

[11] The ratios $N_{LSP}/\Delta CO$, $V_{LSP}/\Delta CO$, $N_{BC}/\Delta CO$, and $M_{BC}/\Delta CO$ were used as indicators of the transport efficiency (TE) of N_{LSP} (TE_{N_LSP}), V_{LSP} (TE_{V_LSP}), N_{BC} (TE_{N_BC}), and M_{BC} (TE_{M_BC}), respectively, during transport from sources to the Arctic. TE values at time t were defined by the following equations.

$$TE_{N_LSP,t} = \frac{[N_{LSP}/\Delta CO]_t}{[N_{LSP}/\Delta CO]_{dry}}, TE_{V_LSP,t} = \frac{[V_{LSP}/\Delta CO]_t}{[V_{LSP}/\Delta CO]_{dry}} \quad (1)$$

$$TE_{N_BC,t} = \frac{[N_{BC}/\Delta CO]_t}{[N_{BC}/\Delta CO]_{dry}}, TE_{M_BC,t} = \frac{[M_{BC}/\Delta CO]_t}{[M_{BC}/\Delta CO]_{dry}}$$

In this equation, $[N_{LSP}/\Delta CO]_t$, $[V_{LSP}/\Delta CO]_t$, $[N_{BC}/\Delta CO]_t$, and $[M_{BC}/\Delta CO]_t$ are the $N_{LSP}/\Delta CO$, $V_{LSP}/\Delta CO$, $N_{BC}/\Delta CO$, and $M_{BC}/\Delta CO$ ratios at time t . The data with $\Delta CO > 20$ ppbv

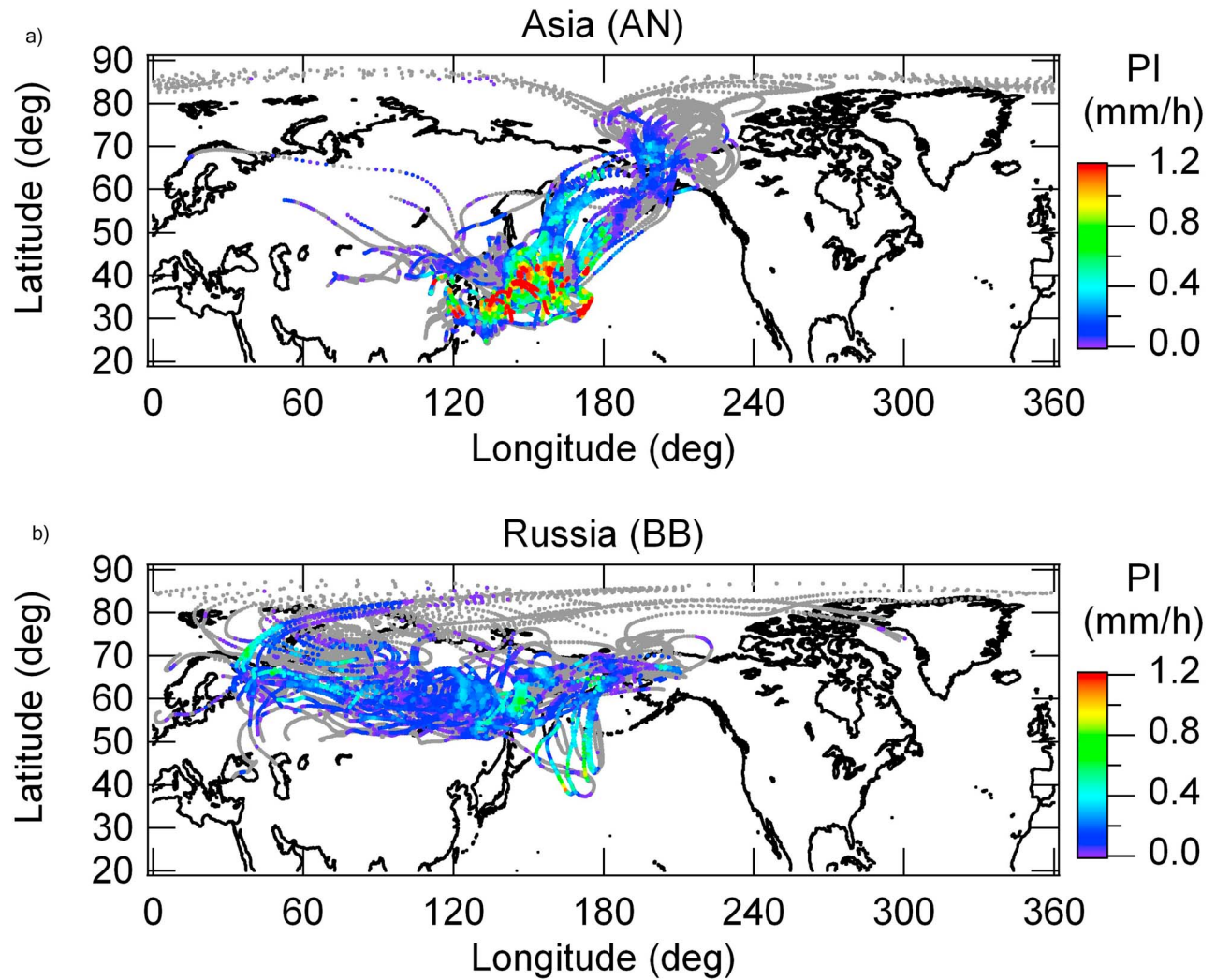


Figure 2. Ten-day backward trajectories for (a) Asian AN and (b) Russian BB air during the ARCTAS-A (spring) campaign. PI denotes precipitation intensity. The periods when $PI < 0.01$ mm/h are shown with gray dots.

were used for the statistical analysis. $[N_{LSP}/\Delta CO]_{dry}$, $[V_{LSP}/\Delta CO]_{dry}$, $[N_{BC}/\Delta CO]_{dry}$, and $[M_{BC}/\Delta CO]_{dry}$ are the ratios for air with a minimum impact of wet removal processes. These dry ratios were estimated using AN and BB air data with $APT < 5$ mm in spring. We used these dry ratios obtained in spring also for summer, because of very limited data with $APT < 5$ mm for summer.

[12] Both numerators and denominators in equation (1) include the increase in V_{LSP} and N_{LSP} by condensation and nucleation processes and the decrease in N_{LSP} and N_{BC} by coagulation processes during transport from sources to the Arctic. Therefore, these processes will partly compensate each other in the TE calculations using equation (1). As a result, we can regard the TE values as a measure of transport efficiency mostly due to removal processes during transport.

[13] We note that the dry ratios for AN air were derived mainly from North American air, because there are few Asian air data with $APT < 5$ mm. The TE values in Asian AN air are likely overestimates, because the dry ratios of $N_{LSP}/\Delta CO$, $V_{LSP}/\Delta CO$, $N_{BC}/\Delta CO$, and $M_{BC}/\Delta CO$ observed in East Asia (A-FORCE aircraft campaign (N. Oshima et al.,

Wet removal of black carbon in Asian outflow: Aerosol Radiative Forcing in East Asia (A-FORCE) aircraft campaign, submitted to *Journal of Geophysical Research*, 2011)) were measured to be about 1.4 times higher than those of AN air estimated in this study.

3. Transport Pathways and Processes of Air Parcels

[14] The transport pathways and processes of measured air parcels have been already analyzed in detail by M2011. Here we briefly summarize their main findings and provide additional results from the viewpoint of the contrast between Asian AN and Russian BB air. During the springtime, most Asian AN air parcels originated from lower latitudes (30° – 40° N) with high relative humidity. They then underwent rapid ascent on the warmer side of cold fronts associated with low-pressure systems and were transported northward and reached the Arctic within a few days after experiencing heavy precipitation and large amounts of latent heating (Figure 2a). These transport pathways are frequently seen in

Table 2. Statistics of Individual Air Parcels During the ARCTAS Campaign

| Source | | Pressure ^a (hPa) | ΔCO^a (ppbv) | N_{LSP}^a (cm^{-3}) | V_{LSP}^a ($\mu\text{m}^3 \text{cm}^{-3}$) | N_{BC}^a (cm^{-3}) | M_{BC}^a (ng m^{-3}) | R_{ORG}^b (%) | $R_{\text{SO}_4}^b$ (%) | $\text{APT}^{a,c}$ (mm) |
|---------------|----------|--------------------------------|-------------------------------|--|--|---|---|---------------------------|----------------------------|----------------------------|
| <i>Spring</i> | | | | | | | | | | |
| Asia | AN | 410 | 32.4 | 25.4 | 0.49 | 2.8 | 18.4 | 24.4 | 66.5 | 23.7 |
| Russia | BB | 608 | 44.1 | 280 | 3.4 | 40.5 | 266 | 61.3 | 25.6 | 8.5 |
| Background | — | 614 | 1.8 | 59.7 | 0.83 | 5.5 | 42.9 | 25.8 | 61.3 | 3.8 |
| <i>Summer</i> | | | | | | | | | | |
| Asia | AN | 353 | 59.1 | 6.2 | 0.051 | 0.33 | 1.4 | 32.9 | 59.0 | 54.9 |
| Russia + Asia | AN | 329 | 78.9 | 4.3 | 0.036 | 0.17 | 0.99 | 48.1 | 43.8 | 30.2 |
| Russia + Asia | BB, ANBB | 466 | 83.8 | 35.5 | 0.43 | 2.1 | 15.8 | 54.9 | 36.4 | 38.5 |
| Russia | BB, ANBB | 527 | 69.6 | 36.4 | 0.40 | 2.1 | 13.6 | 67.8 | 25.4 | 19.0 |
| Background | — | 463 | 1.0 | 15.9 | 0.15 | 1.2 | 5.3 | 54.0 | 39.0 | 10.6 |

^aMedian values are shown for these parameters.

^b R_A denotes the average mass ratio of species A to the total measured submicron mass concentration (non-refractory PM_{10} from the AMS plus BC from the SP2).

^cAPT denotes accumulated precipitation along trajectories.

this region and season and are generally due to warm conveyor belts (WCBs) [e.g., Stohl, 2001; Eckhardt et al., 2003; Oshima et al., 2004; Harrigan et al., 2011; Sessions et al., 2010]. The median APT value was 24 mm for Asian AN air (Table 2). The median transport time from their source (from WCB lifting) to the measurement sites was 7.8 (2.4) days. Since the Asian AN air had relatively high potential temperature at its source and experienced further diabatic heating (due to latent heat release during the WCB ascent), they were generally observed in the UT (300–500 hPa), as shown in Figure 3.

[15] On the other hand, Russian BB air parcels were transported almost isentropically from higher latitudes (50°–70°N), hence they encountered less precipitation and latent heating (Figure 2b). The median APT value was 8.5 mm for Russian BB air (Table 2). The median transport time from their source to the Arctic was 3.5 days. Since Russian BB air had lower potential temperature in the source regions and experienced quasi-adiabatic transport, it was mostly observed in the MT (500–700 hPa) (Figure 3). As a result, the median M_{BC} and $\text{TE}_{\text{M}_{\text{BC}}}$ values were much less for Asian AN air (18 ng m^{-3} and 13%, respectively) than for Russian BB air (266 ng m^{-3} and 83%, respectively).

[16] The median APT during summer was much greater (17 mm) than during spring (3.2 mm) for all flight data used in this study. This was mainly due to the greater precipitation and accompanying wet scavenging over the latitudes 45°–70°N during summer. Correspondingly, the $\text{TE}_{\text{M}_{\text{BC}}}$ values for both Russian BB and Asian AN air were much lower during summer (4.0 and 0.76%, respectively) than during spring (83 and 13%, respectively). The median M_{BC} for all measured air parcels in the Arctic was 5.7 ng m^{-3} , which is 10 times less than during spring (55 ng m^{-3}), while the median ΔCO mixing ratio was somewhat higher than during spring (23 ppbv versus 14 ppbv).

[17] The high $\text{TE}_{\text{M}_{\text{BC}}} - \text{APT}$ correlation ($R^2 = 0.80$ between median values of $\log(\text{TE}_{\text{M}_{\text{BC}}})$ and APT for individual sources and seasons, Figure 13b of M2011), together with the seasonal variations in APT, suggest that the large seasonal variations in M_{BC} were caused mainly by those in the wet removal rates. The contribution of Russian BB in spring to the M_{BC} in the North American Arctic was

largest, because of the spring maximum in $\text{TE}_{\text{M}_{\text{BC}}}$ with low precipitation at higher latitudes.

4. Variation of Accumulation-Mode Aerosol Number Concentration

4.1. Transport Efficiency of N_{LSP} and N_{BC} From Asia to the Arctic

[18] Because the transport and removal processes differed greatly between Asian AN and Russian BB air parcels, as shown in section 3, these processes should also affect the N_{LSP} of individual air parcels. Figure 4 shows the scatterplot between the $N_{\text{LSP}}/\Delta\text{CO}$ ratio and APT for all data (including both source-identified and source-unidentified data) used in this study and that for individual source regions and types (AN and BB). On average, the $N_{\text{LSP}}/\Delta\text{CO}$ ratio decreased with increasing APT in both spring and summer, indicating that removal by precipitation is one of the most important processes in controlling N_{LSP} in the Arctic. This tendency

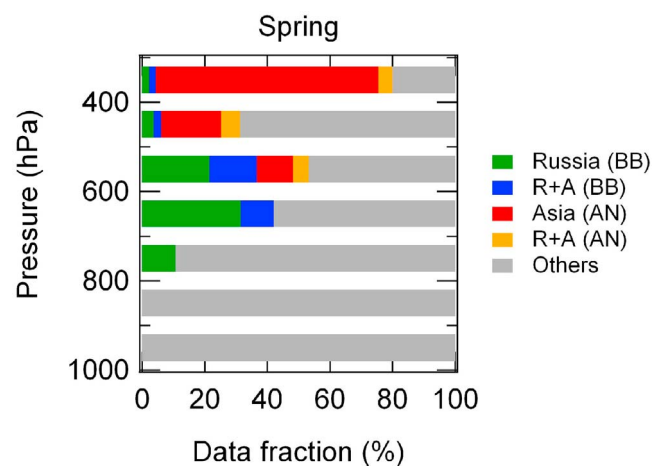


Figure 3. Vertical profile of data number contribution (within the source-identified data) from Russian BB (green), Russia+Asia BB (blue), Asian AN (red), Russia+Asia (orange), and others (gray) during the ARCTAS-A (spring) campaign.

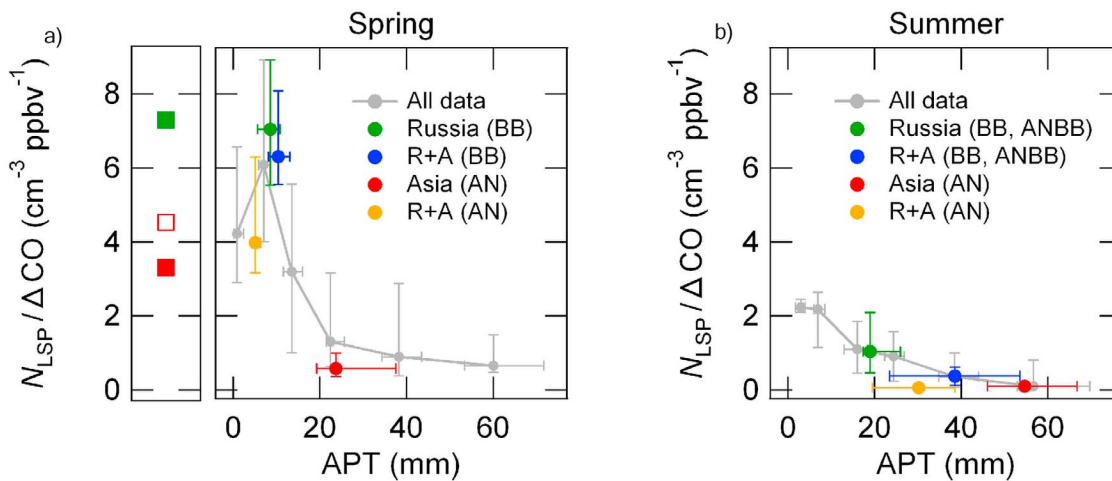


Figure 4. Ratio of number concentrations of light-scattering particles (N_{LSP}) and ΔCO as a function of accumulated precipitation along trajectories (APT) for both (a) spring and (b) summer. The medians (circles) and 25th–75th percentiles (vertical and horizontal bars) are shown. The squares in Figure 4a (left) show the median dry ratio of $N_{LSP}/\Delta CO$ for the anthropogenic (AN, closed red) and biomass burning (BB, closed green) sources, which were estimated from AN and BB air parcels with APT < 5 mm and for the AN source in East Asia estimated from the A-FORCE aircraft campaign (open red), respectively. “All data” includes both the source-identified and source-unidentified data.

does not change even if Russian BB and Asian AN data are excluded. The $N_{LSP}/\Delta CO$ ratio was low at high APT values for Asian AN air, which was mostly measured in the UT. In contrast, the $N_{LSP}/\Delta CO$ ratio was much higher for Russian BB air parcels, which were mainly transported to the Arctic MT with low APT (sections 3 and 4.2). These results are similar to those for M_{BC} discussed in M2011.

[19] Figures 5a and 5b show that N_{LSP} and N_{BC} had high correlations for all the data used in this study (gray dots in Figures 5a and 5b) during both spring ($R^2 = 0.87$) and summer ($R^2 = 0.57$). The median N_{LSP} and N_{BC} in spring were 25.4 and 2.8 cm^{-3} for Asian AN air, 280 and 40.5 cm^{-3} for Russian BB air, and 79.6 and 7.5 cm^{-3} for all the data for spring used in this study, respectively (Table 2). The lower number concentrations (both LSP and BC) in Asian AN air were due to the effective wet scavenging of aerosols during WCB transport, and the higher concentrations in Russian BB air were due to the efficient transport of aerosols. The number concentrations (both LSP and BC) during summer were systematically less than those during spring. This was mainly due to the greater precipitation over the latitudes 45°–70°N in summer (section 3 and M2011). The median values of N_{LSP} and N_{BC} in summer were 6.2 and 0.33 cm^{-3} for Asian AN air, 36.4 and 2.1 cm^{-3} for Russian BB and ANBB air, and 18.6 and 1.2 cm^{-3} for all the data for summer, respectively (Table 2). Similar good correlation and seasonal variation was found between V_{LSP} and M_{BC} ($R^2 = 0.87$ for spring and $R^2 = 0.73$ for summer). The N_{LSP}/N_{BC} ratio was a factor of 2–4 higher during summer than spring for individual sources (Table 2). This seasonal variation is qualitatively consistent with surface measurements of aerosol optical properties at Barrow [Quinn *et al.*, 2002]. Since the number of data used in this study is very limited especially during summer (two flights), further studies are needed to understand whether this seasonality is general in the Arctic, including MT and UT.

[20] Figure 5c shows the correlation between median values of $TE_{N_{LSP}}$ and $TE_{N_{BC}}$ for individual source regions and types in both spring (closed circles) and summer (open squares). The median TE values were highly correlated with $R^2 = 0.88$ (Figure 5c). Due to the differences in transport and removal processes, the median $TE_{N_{LSP}}$ and $TE_{N_{BC}}$ values were much greater for Russian BB air (97 and 85%, respectively) than for Asian AN air (18 and 18%, respectively) in spring. In addition, TE values during spring were systematically higher than those in summer (Figure 5c and Table 3). These variations in TE are similar to those in $TE_{M_{BC}}$ (M2011). The median $TE_{V_{LSP}}$ and $TE_{M_{BC}}$ were also highly correlated ($R^2 = 0.90$) (Figure 5d). The $TE_{V_{LSP}}/TE_{M_{BC}}$ ratio for summer was higher than during spring (Figures 5c and 5d and Table 3). This is consistent with the N_{LSP}/N_{BC} ratio because we used the same dry ratio (the $N_{LSP}/\Delta CO$, $V_{LSP}/\Delta CO$, $N_{BC}/\Delta CO$, and $M_{BC}/\Delta CO$ ratios with APT < 5 mm) for summer and spring to derive the TE values for summer (section 2.2 and M2011). The dry ratios in summer might be higher than during spring in the real atmosphere due to faster growth and formation rates of LSP by a higher oxidation rate during transport.

[21] N_{LSP} , V_{LSP} , N_{BC} , and M_{BC} and their TE values were tightly correlated (Figure 5), indicating that LSP and BC had similar or collocated (at the horizontal scale of this study) emission sources and experienced similar levels of removal processes for both number and volume concentrations (>180 nm) during transport from their sources to the Arctic. We interpret similar TE values between LSP and BC as due to sufficient processing of BC during transport, resulting in hygroscopicity as high as that of LSP particles. This interpretation is supported by the long transport time from sources to the Arctic (section 3) and observed thick coatings of BC particles. Specifically, the median value of the shell (LSP + BC) to core (BC) diameter ratio in spring was 1.51 and 1.35

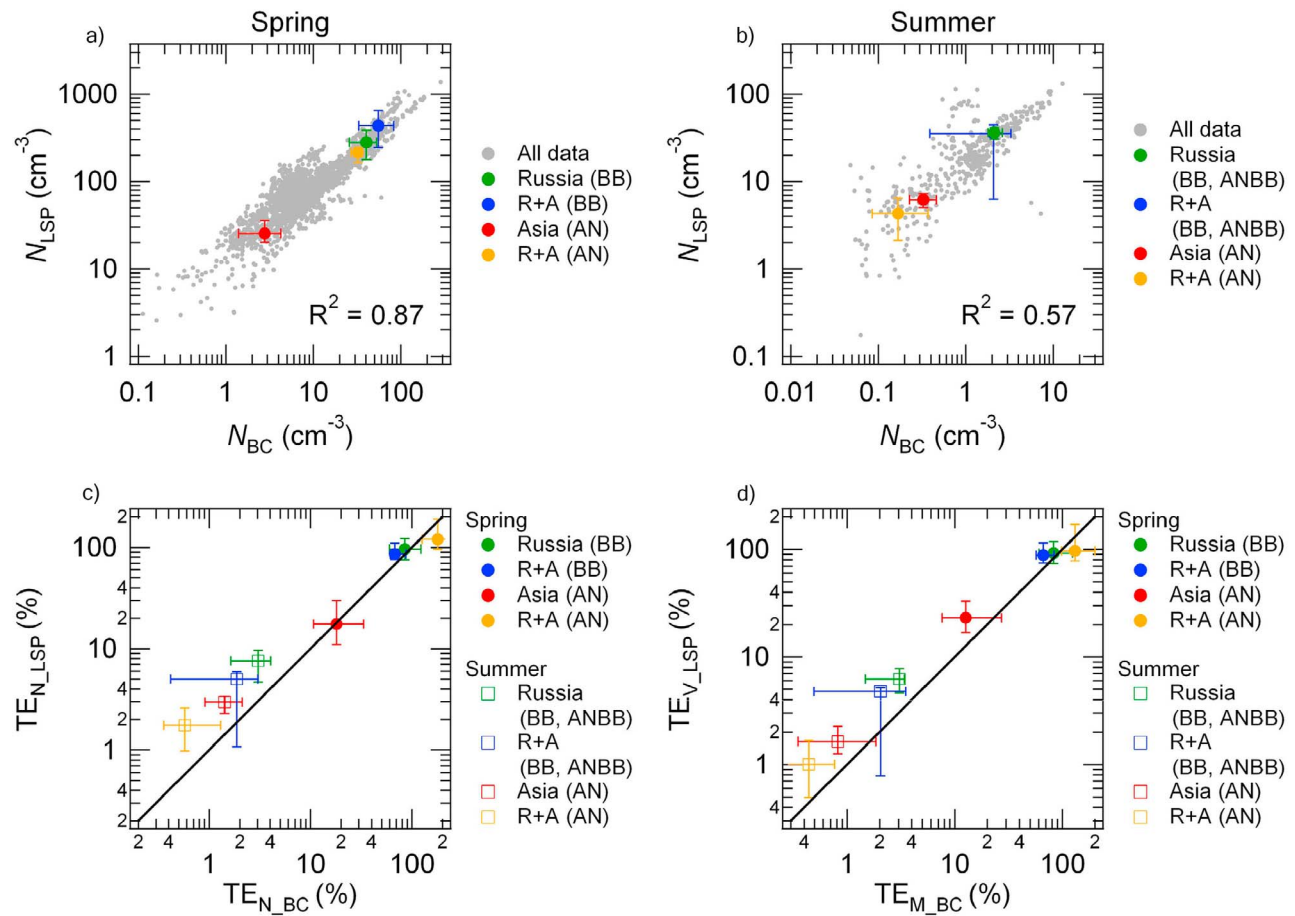


Figure 5. Correlation between number concentrations of light-scattering particles (N_{LSP}) and black carbon (N_{BC}) in (a) spring and (b) summer for all data used in this study (gray) and individual sources (colors). Correlation between (c) transport efficiencies of N_{LSP} (TE_{N_LSP}) and N_{BC} (TE_{N_BC}) and (d) those of V_{LSP} (TE_{V_LSP}) and M_{BC} (TE_{M_BC}) in spring (closed circles) and summer (open squares). Medians and 25th–75th percentiles are shown for individual sources.

Table 3. Transport Efficiency (TE) and Fractional Contribution (F) of Individual Air Parcels During the ARCTAS Campaign

| Source | | $TE_{N_LSP}^a$ (%) | $TE_{V_LSP}^a$ (%) | $TE_{N_BC}^a$ (%) | $TE_{M_BC}^a$ (%) | $F_{N_LSP}^b$ (%) | $F_{V_LSP}^b$ (%) | $F_{N_BC}^b$ (%) | $F_{M_BC}^b$ (%) |
|---------------------|----------|------------------------|------------------------|-----------------------|-----------------------|-----------------------|-----------------------|----------------------|----------------------|
| <i>Spring</i> | | | | | | | | | |
| Asia | AN | 17.5 | 23.3 | 18.0 | 12.6 | 2.7 | 3.4 | 2.0 | 2.2 |
| Russia | BB | 96.5 | 92.1 | 85.1 | 82.6 | 27.3 | 26.7 | 28.1 | 28.0 |
| Russia + Asia | BB | 86.4 | 88.3 | 67.6 | 66.2 | 19.0 | 19.7 | 18.3 | 18.0 |
| Russia + Europe | BB | 88.1 | 87.7 | 80.0 | 74.3 | 13.4 | 13.7 | 13.5 | 13.2 |
| Others ^c | — | — | — | — | — | 37.6 | 36.5 | 38.1 | 38.6 |
| <i>Summer</i> | | | | | | | | | |
| Asia | AN | 3.0 | 1.6 | 1.4 | 0.82 | 8.4 | 6.8 | 8.9 | 9.0 |
| Russia + Asia | AN | 1.8 | 1.0 | 0.57 | 0.44 | 17.0 | 15.1 | 13.4 | 11.2 |
| Russia + Asia | BB, ANBB | 5.0 | 4.8 | 1.9 | 2.1 | 16.8 | 17.3 | 18.4 | 22.6 |
| Russia | BB, ANBB | 7.6 | 6.2 | 3.1 | 3.1 | 33.3 | 33.7 | 33.9 | 32.8 |
| Others ^c | — | — | — | — | — | 24.5 | 27.1 | 25.4 | 24.4 |

^aTE denotes transport efficiency defined by equation (1).

^bF denotes the fractional contributions of individual sources to the total concentrations in the North American Arctic (sum of the concentration for all source-identified data) defined by equation (2).

^cOthers denotes source-identified data from other sources (Europe, Russia (AN), Russia + Europe, Russia + Asia, Asia (BB), and North America), which were defined and used by M2011.

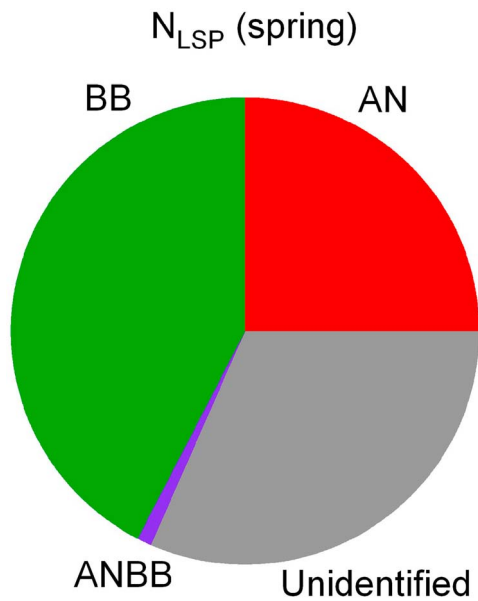


Figure 6. Contribution from biomass burning (BB) and anthropogenic (AN) sources to the total N_{LSP} concentrations within all the data during the ARCTAS-A (spring) campaign.

for Russian BB and Asian AN air, respectively, for a core diameter of 200 nm, although it should be noted that measured particles were not scavenged during transport but survived wet removal processes.

[22] We calculated the contributions of individual sources to the total N_{LSP} , V_{LSP} , N_{BC} , and M_{BC} in the North American Arctic (sum of the measured concentration for all source-identified data) using the following equations (2).

$$F_{N_LSP,i} = \frac{\sum_j N_{LSP,i,j}}{\sum_j N_{LSP,j,i}}, \quad F_{V_LSP,i} = \frac{\sum_j V_{LSP,i,j}}{\sum_j V_{LSP,j,i}} \quad (2)$$

$$F_{N_BC,i} = \frac{\sum_j N_{BC,i,j}}{\sum_j N_{BC,j,i}}, \quad F_{M_BC,i} = \frac{\sum_j M_{BC,i,j}}{\sum_j M_{BC,j,i}}$$

$F_{N_LSP,i}$, $F_{V_LSP,i}$, $F_{N_BC,i}$, and $F_{M_BC,i}$ are the fractional contribution of source i to the total amount of N_{LSP} , V_{LSP} , N_{BC} , and M_{BC} , respectively. $N_{LSP,i,t}$, $V_{LSP,i,t}$, $N_{BC,i,t}$, and $M_{BC,i,t}$ are N_{LSP} , V_{LSP} , N_{BC} , and M_{BC} at time t from source i , respectively, while j means summation of the values for all sources. The fractional contribution of N_{LSP} , V_{LSP} , N_{BC} , and M_{BC} for BB air that passed over Russia (sum of BB and ANBB sources from Russian, Russia + Asia, and Russia + Europe) was as high as 60% in spring and 66% in summer (Table 3), indicating that Russian BB was the dominant source of aerosol (for both LSP and BC and for both number and volume concentrations) within the source-identified data. In contrast, the fractional contribution from Asian AN air was as low as 2–3% in spring and 7–9% in summer within the source-identified data (Table 3), indicating the very limited impact from Asian AN sources on Arctic aerosol.

[23] The contribution from BB and AN sources (including data of unidentified source regions) to all the data (both

source-identified and source-unidentified data) in spring was estimated to be 42–48% and 25–27%, respectively, for N_{LSP} , V_{LSP} , N_{BC} , and M_{BC} (the remainder is data of unidentified source types) (Figure 6). This result suggests that BB emissions were the primary source of aerosol (for both LSP and BC and for both number and volume concentrations) in the North American Arctic in spring 2008. Although the source regions were not identified for more than 50% of the data in BB by trajectory calculations, most BB-influenced air probably originated from Russia and Kazakhstan considering that few data were from other BB sources within the source-identified data during spring (Table 2 of M2011).

[24] In summary, Russian BB in spring was the most important source of accumulation-mode aerosols over the Arctic for both LSP and BC and for both number and volume concentrations during the ARCTAS campaign within the source-identified data. BB emissions were found to be the primary source of aerosol within all the data in spring during ARCTAS. In contrast, Asian AN air provided a negligible contribution to the accumulation-mode aerosols (both LSP and BC) over the North American Arctic in both spring and summer 2008.

4.2. Vertical Profile of N_{LSP}

[25] Figure 7 shows the vertical profiles of N_{LSP} measured during spring and summer. N_{LSP} had a broad maximum in the MT in spring. This profile is similar to that of M_{BC} shown in M2011. We can interpret this vertical profile by the differences in TE_{N_LSP} (Figure 5c and Table 3) and the differences in altitude profiles (Figure 3) between the Asian AN and Russian BB air parcels. The broad peak in the MT was due to the dominant contribution of Russian BB. The decrease in the UT was due to efficient wet removal of LSP in Asian AN air. The shapes of the vertical profiles of V_{LSP} and N_{BC} were similar to that of N_{LSP} (not shown).

4.3. Comparison of N_{LSP} With Background Aerosol Concentrations

[26] The values of N_{LSP} in Asian AN and Russian BB air were compared with those of background air. We defined background air as source regions that were not identified (not from Europe, Russia, Asia, or North America) based on trajectory calculations and had concentrations of ΔCO , ΔCH_3CN , and ΔCH_2Cl_2 that were less than 5 ppbv, 50 pptv, and 5 pptv, respectively. Compared with background air, the median N_{LSP} for Russian BB air were factors of 4.7 and 2.3 greater during spring and summer, respectively, while those of Asian AN air were factors of 2.4 and 2.6 smaller in spring and summer, respectively (Figure 8 and Table 2). These features were also seen for V_{LSP} , N_{BC} , and M_{BC} (Table 2). This result indicates that inflow of midlatitude Asian AN air decreased aerosol concentrations in the Arctic (cleansing effect). The high concentrations of ΔCO (levels similar to Russian BB air) for AN air suggest high concentrations of aerosols and their precursors in the source region.

[27] WCBs are a common synoptic-scale transport mechanism over various regions at midlatitudes and seasons [Stohl, 2001; Eckhardt *et al.*, 2003]. Aerosol concentrations in air transported via this mechanism from midlatitudes will generally be lower than that in background Arctic air. This process can be one of the most important processes in controlling aerosol concentrations in the MT and UT in the

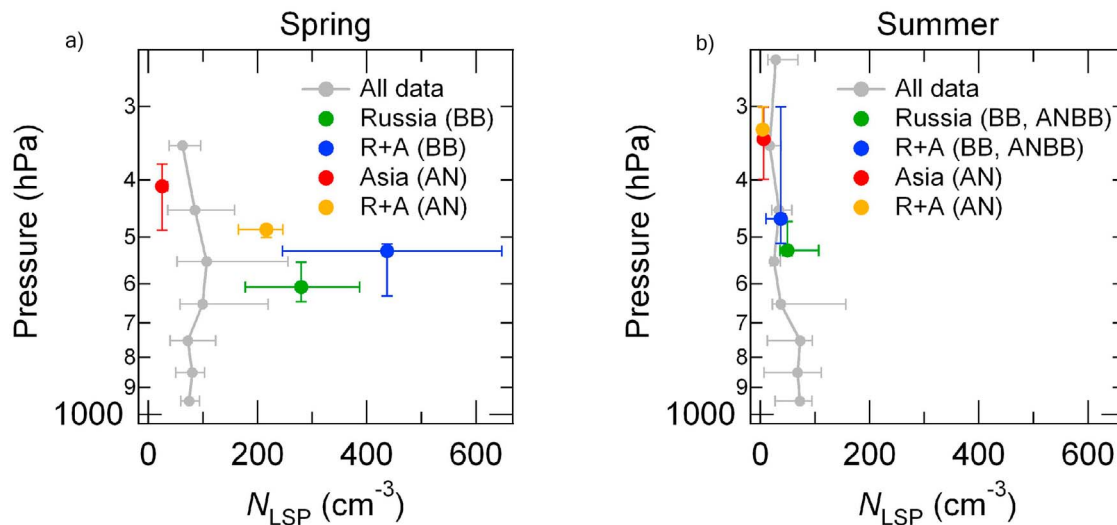


Figure 7. Median vertical profiles in (a) spring and (b) summer for all data used in this study (gray) and individual sources (colors). Horizontal bars denote 25th–75th percentiles.

Arctic in spring and summer. Further studies, especially using chemical transport models, are needed to assess the effect more quantitatively, including the frequency of inflow of clean midlatitude air to the Arctic.

4.4. Chemical Composition of LSP

[28] Asian AN and Russian BB air also had marked differences in aerosol chemical composition. The average mass ratio of sulfate aerosol to the total PM_{10} mass concentrations (R_{SO_4}) was largest (67% in spring and 59% in summer) in Asian AN air, while that of organic aerosol (R_{ORG}) was largest (61% in spring and 68% in summer) in Russian BB air during both spring and summer (Table 2 and Figure 9). This reflects characteristics of the emissions of trace gases and aerosols in the Asian continent. In fact, based on emission inventories for the Asian continent, the mass emission ratio between SO_2 and primary organic carbon is about 1–2 orders of magnitude greater for anthropogenic sources in Asia

(7.2, SO_2 dominant) [Zhang *et al.*, 2009] than for biomass burning sources in East Asia (0.11, organic carbon dominant) [Streets *et al.*, 2003], although the relative contribution of secondary organic aerosol formation during transport might be larger for AN air than BB air [Cubison *et al.*, 2011]. The sulfate mass fraction was as large as about 30% in Russian BB air (Table 2 and Figure 9). Sulfate in Russian BB air could be from SO_2 emission from fires in the flaming phase and their oxidation to sulfate [Kondo *et al.*, 2011] and mixing with background air, which includes high fractions of sulfate (Table 2 and Figure 9c).

[29] The background air parcels in spring had chemical compositions similar to Asian AN air (high sulfate/organics ratio), suggesting that they could have been influenced mainly by AN sources (Figure 9c). On the other hand, the background air in summer had a greater fraction of organics (Figure 9f), suggesting that they had been influenced by both AN and BB sources. This result implies that Arctic background

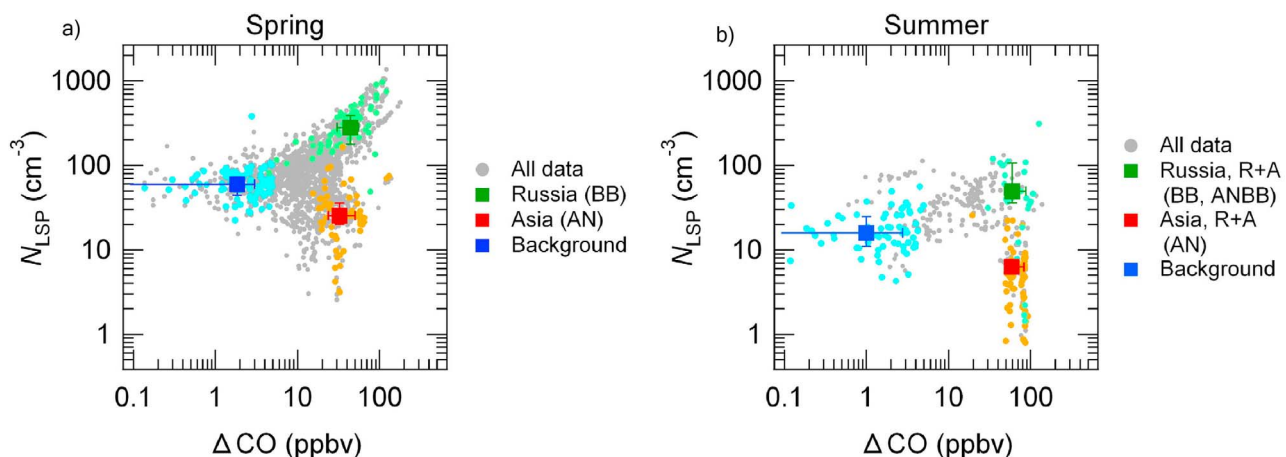


Figure 8. Scatterplots of N_{LSP} and ΔCO in (a) spring and (b) summer. Gray dots and circles denote 1-min data used in this study. Squares and bars show the medians and 25th–75th percentiles of Asian AN (red), Russian BB (green), and background (blue) air parcels.

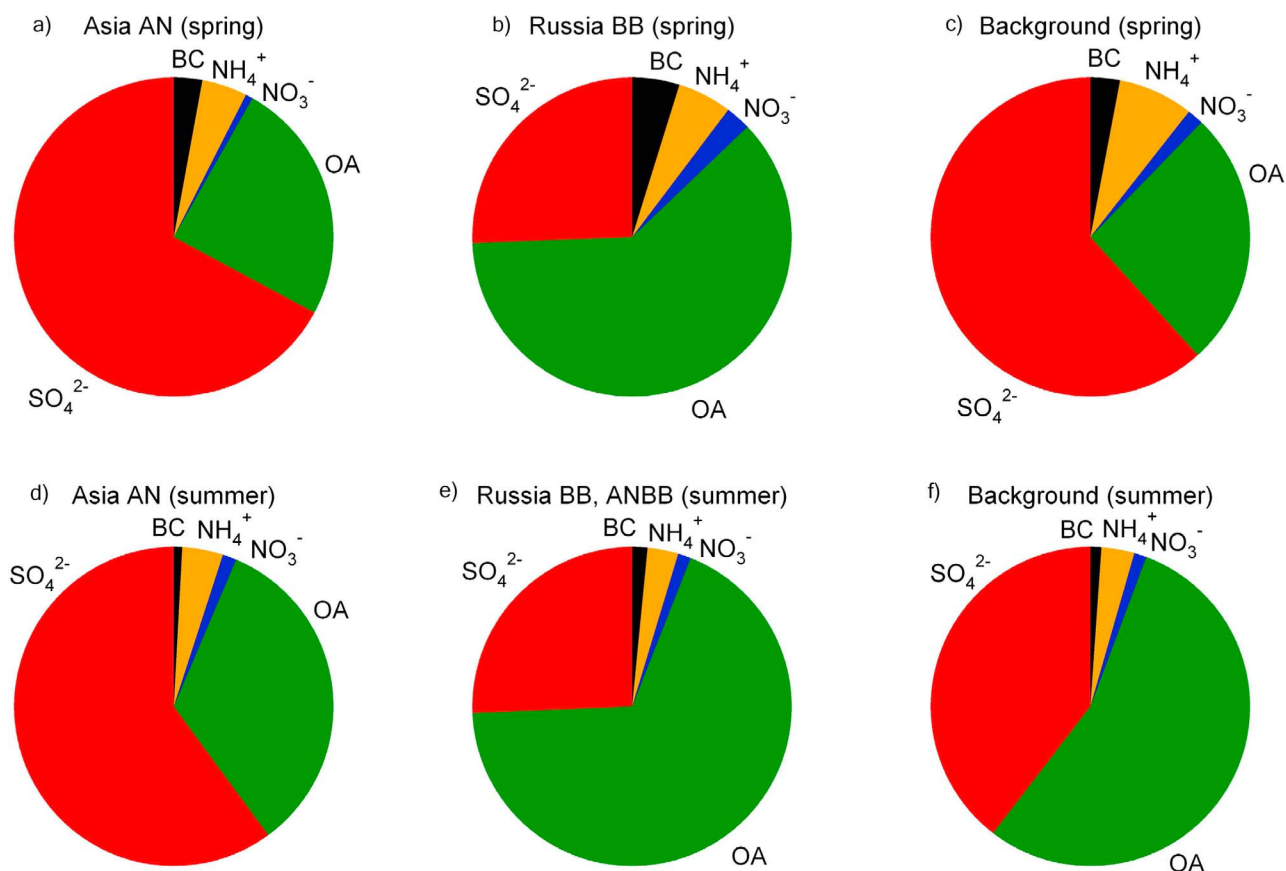


Figure 9. Average chemical composition (mass ratio) in (a, b, c) spring and (d, e, f) summer for Asian AN (Figures 9a and 9d), Russian BB (Figures 9b and 9e), and background air parcels (Figures 9c and 9f).

aerosols during winter and early spring are mainly from AN sources, while BB emissions taking place from spring to summer may alter aerosol concentrations and chemical compositions in the Arctic by summer.

[30] Chemical compositions (average mass ratio) in spring shown in Figure 9 are generally consistent with the measurements during the Aerosol, Radiation, and Cloud Processes affecting Arctic Climate (ARCPAC) aircraft campaign in spring 2008 [Brock *et al.*, 2011]. Both studies showed that organics were dominant (about 60% of fine particles) for BB air parcels and comprised 20–30% of fine particles for AN air parcels. The contribution of sulfate in background air was slightly higher during ARCTAS (about 60%) than ARCPAC (about 50%). The contribution of BC was about 3–5% of fine particles for all air parcels.

4.5. Size Distribution of LSP

[31] Asian AN and Russian BB also exhibit marked differences in the normalized size distribution of V_{LSP} (Figure 10), which is defined for all one-minute data as the size distribution of V_{LSP} normalized by the total V_{LSP} : Russian BB air had nearly a single lognormal distribution with a peak diameter of 250 nm, while Asian AN air had a two-mode lognormal distribution with peak diameters of 250 and 530 nm (although the absolute concentrations were an order of magnitude less than Russian BB air, as shown

in Table 2). The widths of size distributions were narrow for both N_{LSP} (1.20–1.23) and V_{LSP} (1.24–1.30) for both Russian BB and Asian AN air. These standard deviations are generally consistent with those calculated from the peak diameters of number and volume size distributions when lognormal distributions are assumed. Compared with Brock *et al.* [2011], our measurements during spring had greater peak diameters of number size distributions and smaller peak diameters of volume size distributions and standard deviations for all air parcels.

[32] The larger mode of Asian AN air is possibly due to aqueous-phase aerosol growth within cloud droplets during transport. The dispersions of the size distribution (vertical bars in Figure 10a) for Asian AN air were larger than for Russian BB air (Figure 10b) for LSP. These results are consistent with a stronger impact of wet removal processes for Asian AN air. In addition to the aqueous-phase growth, mixing with background air, which contained moderate concentrations of larger particles (Figure 10c), could be a source of the larger mode of Asian AN air. Dust particles might be another potential source of larger particles [Leitch *et al.*, 2009; McKendry *et al.*, 2011], but the median volume concentrations of coarse particles derived by APS ($0.12 \mu\text{m}^3 \text{cm}^{-3}$) were considerably smaller compared with those of the accumulation mode derived by SP2 ($0.49 \mu\text{m}^3 \text{cm}^{-3}$) for Asian AN air parcels during spring. The contribution from mixing of BB

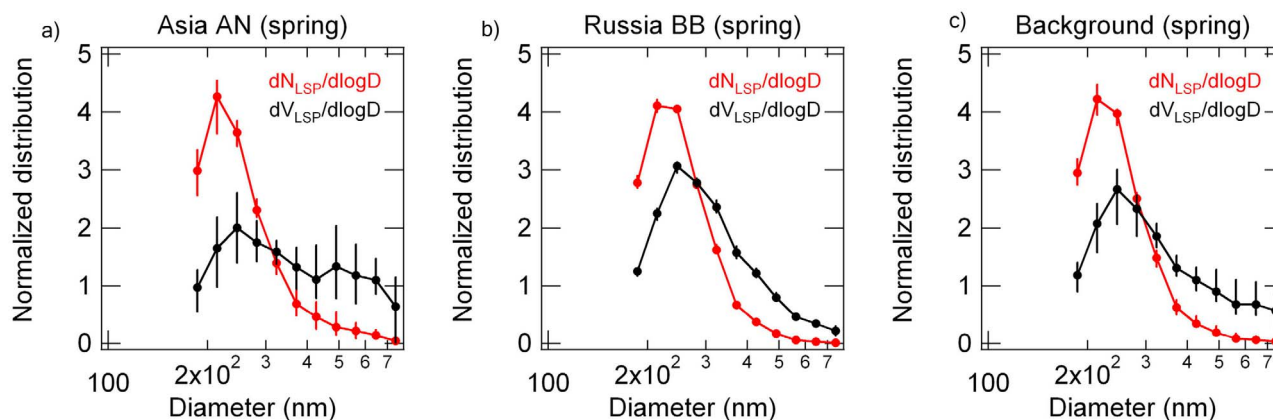


Figure 10. Medians and 25th–75th percentiles of normalized size distribution of N_{LSP} (red) and V_{LSP} (black) for (a) Asian AN, (b) Russian BB, and (c) background air parcels in spring. Normalized number and volume size distributions are the size distribution normalized by the total number and volume concentrations of LSP, respectively, and are calculated for individual one-min data.

air to Asian AN air should be limited for both smaller and larger modes because of the strict criteria for choosing Asian AN air (low concentrations of ΔCH_3Cl).

[33] Finally, we note that total aerosol number concentrations (N_{CPC}) and N_{LSP} exhibited very different variations during ARCTAS. The median N_{LSP}/N_{CPC} ratio for Asian AN (Russian BB) air was 0.08 (0.53) in spring and 0.05 (0.09) in summer during ARCTAS. The Aitken and nucleation-mode particles were dominant when the accumulation-mode particles were low, suggesting that new particle formation might have occurred in these air parcels during transport after the wet scavenging of accumulation-mode particles. This tendency is consistent with previous measurements of air transport from Asian sources [Brock *et al.*, 2004; Dunlea *et al.*, 2009; Weber *et al.*, 2003].

5. Potential of Aerosol-Cloud Interaction

[34] We briefly discuss the potential impacts of the transport of polluted (Russian BB) and clean (Asian AN) air on aerosol-cloud interactions in the Arctic, based on the findings of recent studies. The median N_{LSP} of Russian BB air was 280 cm^{-3} in spring. Lubin and Vogelmann [2006] estimated a longwave aerosol indirect effect (AIE) of 3.4 W m^{-2} for Arctic stratus clouds, which contain aerosol number concentrations greater than 175 cm^{-3} . Assuming a case in which Russian BB air forms stratus clouds in the Arctic, they could have an equivalent or greater potential of cloud-radiation feedback (longwave indirect warming effect) than that presented by Lubin and Vogelmann [2006].

[35] On the other hand, when shortwave AIE is included, the total (longwave + shortwave) first AIE can be positive during early spring (March–April) but negative in late spring and summer (April–July) [Lubin and Vogelmann, 2010; Alterskjær *et al.*, 2010] because shortwave solar radiation increases with the progression of the seasons. Longwave and shortwave AIEs will generally compensate for each other in spring. The onset of BB in Russia in 2008 corresponds to the transition period from positive to negative total first AIE. An earlier onset of Russian BB in the future [Stocks *et al.*, 1998]

may contribute to an additional Arctic warming by the total first AIE.

[36] Some studies suggest that the entrainment of CCN and ice nuclei into Arctic stratus clouds in the LT can contribute to increases in cloud droplet number, liquid water path, and cloud optical depth [Jiang *et al.*, 2001], and possibly affect the acceleration of snow-ice melting [Carrió *et al.*, 2005a, 2005b]. Russian BB aerosols in the MT have the potential to be entrained into the BL and could contribute to Arctic warming by this effect and resulting dynamical changes. Since Russian BB air may have both warming (longwave AIE and entrainment of ML air to the BL) and cooling (shortwave AIE) effects, as shown above, more detailed studies are needed to understand the relative importance of the individual effects quantitatively.

[37] Since Asian AN air had lower N_{LSP} than background air, these air parcels may cause opposite aerosol indirect effects through the reduction of cloud emissivity and lifetime (compared with background air). In addition, since the median N_{LSP} of Asian AN air was only 6.2 cm^{-3} in summer, cloud formation and precipitation processes (if we assume a case with supersaturated conditions) could be limited by the available CCN concentration, as proposed by Mauritsen *et al.* [2011]. This cloud regime may cause higher supersaturation, increase precipitation efficiency, cause a positive feedback on the aerosol by increased wet deposition, and produce lower aerosol concentrations in the Arctic [Mauritsen *et al.*, 2011]. Therefore, Asian AN may have additional cleansing effects by this aerosol-cloud-precipitation interaction in the Arctic if this effect could be applied to the UT.

6. Summary

[38] We have evaluated the impacts of transport of mid-latitude air on aerosol number concentrations in the accumulation mode (light scattering particles (LSP) with diameters $>180 \text{ nm}$, N_{LSP}) in the Arctic during the ARCTAS aircraft campaign conducted in April and June–July 2008. We focused on air parcels transported from anthropogenic sources in East Asia (Asian AN) and biomass burning sources in Russia and

Kazakhstan (Russian BB). Most Asian AN air parcels were transported from lower latitudes (30°–40°N) and had fairly high relative humidity. They experienced rapid ascent by warm conveyor belts (WCBs) with heavy precipitation, while Russian BB air parcels were transported almost isentropically from higher latitudes (50°–70°N) and encountered less precipitation.

[39] Due to these differences in transport processes, we found marked differences in the number concentration (N_{LSP}), transport efficiency ($TE_{N_{LSP}}$), size distribution, and chemical composition of aerosols between Asian AN and Russian BB air. Asian AN air had lower N_{LSP} and $TE_{N_{LSP}}$ (25 cm⁻³ and 18% in spring and 6.2 cm⁻³ and 3.0% in summer) than Russian BB air (280 cm⁻³ and 97% in spring and 36 cm⁻³ and 7.6% in summer) due to more intense wet scavenging during transport from Asia. N_{LSP} and $TE_{N_{LSP}}$ in summer were much lower than those in spring for both sources. Russian BB air had nearly a single lognormal distribution of aerosol volume concentrations (V_{LSP}) with a peak diameter of 250 nm, while Asian AN air had a two-mode lognormal distribution with peak diameters of 250 and 530 nm. The size distribution was narrow (standard deviation of 1.2–1.3) for both Russian BB and Asian AN air. The second peak of V_{LSP} in Asian AN air is likely droplet-mode aerosols, which are consistent with WCB transport with efficient cloud and precipitation processes. Sulfate and organic aerosols were dominant in Asian AN and Russian BB air, respectively, reflecting emission sources. The chemical compositions of background air parcels suggest that they were mainly influenced by AN sources in spring and both AN and BB sources in summer. This result implies that BB emissions from spring to summer alter aerosol concentrations and chemical compositions in the Arctic.

[40] N_{LSP} , V_{LSP} , and number and mass concentrations of BC and their TE values were tightly correlated, indicating that LSP and BC were sufficiently processed and had experienced similar levels of removal processes during transport from their sources to the Arctic. Within the source-identified data, Russian BB in spring was the largest and most important source of accumulation-mode aerosols for both LSP and BC and for both number and volume concentrations during the ARCTAS campaign (60–70% of total accumulation-mode aerosols). On the other hand, the transport of Asian AN air contributed little to both LSP and BC in the Arctic in spring and summer (less than 10% of total accumulation-mode aerosols). The contribution from BB and AN sources to all the data (both source-identified and source-unidentified data) in spring was estimated to be 42–48% and 25–27%, respectively, for N_{LSP} , V_{LSP} , N_{BC} , and M_{BC} , suggesting that BB emissions were the primary source of aerosol (for both LSP and BC and for both number and volume concentrations) in the North American Arctic in spring 2008.

[41] The median N_{LSP} of Russian BB air were factors of 4.7 and 2.3 higher than those of background air in spring and summer, respectively, while those of Asian AN air were factors of 2.4 and 2.6 lower than those of background air in spring and summer, respectively. The latter was due to wet removal during WCB transport and indicates that Asian AN air can reduce aerosol concentrations in the Arctic (cleansing effect). Since WCBs are a common synoptic-scale transport mechanism over the midlatitudes, it is expected that the transport of midlatitude air can be a source of clean air (in

terms of aerosols) in the Arctic in spring and summer. Further studies are needed to quantify this effect on the climate of the Arctic.

[42] **Acknowledgments.** The ARCTAS campaign was supported by NASA. We are indebted to all the ARCTAS participants for their cooperation and support. Special thanks are due to the flight and ground crews of the NASA DC-8 aircraft. We thank M. Osuka for his assistance with the field measurements. This work was supported in part by the Ministry of Education, Culture, Sports, Science, and Technology (MEXT), the strategic international cooperative program of the Japan Science and Technology Agency (JST), and the global environment research fund of the Japanese Ministry of the Environment (A1101). Y.Z. was supported in part by NASA's Tropospheric Chemistry Program (USP-SMD-08-009). CH₃CN measurements were supported by the Austrian Research Promotion Agency (FFG-ALR) and the Tiroler Zukunftstiftung and were carried out with the help/support of T. Mikoviny, M. Graus, A. Hansel, and T. D. Maerk. M.J.C. and J.L.J. were supported by NASA NNX08AD39G.

References

- Adler, R. F., et al. (2003), The Version 2 Global Precipitation Climatology Project (GPCP) monthly precipitation analysis (1979–Present), *J. Hydrometeorol.*, **4**, 1147–1167, doi:10.1175/1525-7541(2003)004<1147:TVGPCP>2.0.CO;2.
- Alterskjær, K., J. E. Kristjánsson, and C. Hoose (2010), Do anthropogenic aerosols enhance or suppress the surface cloud forcing in the Arctic?, *J. Geophys. Res.*, **115**, D22204, doi:10.1029/2010JD014015.
- Anderson, B. E., W. R. Cofer, D. R. Bagwell, J. W. Barrick, C. H. Hudgins, and K. E. Brunke (1998), Airborne observations of aircraft aerosol emissions: 1. Total and nonvolatile emission indices, *Geophys. Res. Lett.*, **25**(10), 1689–1692, doi:10.1029/98GL00063.
- Barrie, L. A. (1986), Arctic air pollution: An overview of current knowledge, *Atmos. Environ.*, **20**, 643–663, doi:10.1016/0004-6981(86)90180-0.
- Blake, N. J., et al. (2003), NMHCs and halocarbons in Asian continental outflow during the Transport and Chemical Evolution over the Pacific (TRACE-P) field campaign: Comparison with PEM-West B, *J. Geophys. Res.*, **108**(D20), 8806, doi:10.1029/2002JD003367.
- Brock, C. A., L. F. Radke, and P. V. Hobbs (1990), Sulfur in particles in Arctic hazes derived from airborne in situ and lidar measurements, *J. Geophys. Res.*, **95**(D13), 22,369–22,387, doi:10.1029/JD095iD13p22369.
- Brock, C. A., et al. (2004), Particle characteristics following cloud-modified transport from Asia to North America, *J. Geophys. Res.*, **109**, D23S26, doi:10.1029/2003JD004198.
- Brock, C. A., et al. (2011), Characteristics, sources, and transport of aerosols measured in spring 2008 during the aerosol, radiation, and cloud processes affecting Arctic Climate (ARCPAC) Project, *Atmos. Chem. Phys.*, **11**, 2423–2453, doi:10.5194/acp-11-2423-2011.
- Carrió, G. G., H. Jiang, and W. R. Cotton (2005a), Impact of aerosol intrusions on Arctic boundary layer clouds, part I: 4 May 1998 case, *J. Atmos. Sci.*, **62**, 3082–3093, doi:10.1175/JAS3454.1.
- Carrió, G. G., H. Jiang, and W. R. Cotton (2005b), Impact of aerosol intrusions on Arctic boundary layer clouds, part II: Sea ice melting rates, *J. Atmos. Sci.*, **62**, 3094–3105, doi:10.1175/JAS3558.1.
- Chen, M., R. Talbot, H. Mao, B. Sive, J. Chen, and R. J. Griffin (2007), Air mass classification in coastal New England and its relationship to meteorological conditions, *J. Geophys. Res.*, **112**, D10S05, doi:10.1029/2006JD007687.
- Cubison, M. J., et al. (2011), Effects of aging on organic aerosol from open biomass burning smoke in aircraft and lab studies, *Atmos. Chem. Phys. Discuss.*, **11**, 12,103–12,140, doi:10.5194/acpd-11-12103-2011.
- DeCarlo, P. F., et al. (2006), Field-deployable, high-resolution, time-of-flight aerosol mass spectrometer, *Anal. Chem.*, **78**, 8281–8289, doi:10.1021/ac061249n.
- Dunlea, E. J., et al. (2009), Evolution of Asian aerosols during transpacific transport in INTEX-B, *Atmos. Chem. Phys.*, **9**, 7257–7287, doi:10.5194/acp-9-7257-2009.
- Eckhardt, S., A. Stohl, S. Beirle, N. Spichtinger, P. James, C. Forster, C. Junker, T. Wagner, U. Platt, and S. G. Jennings (2003), The North Atlantic Oscillation controls air pollution transport to the Arctic, *Atmos. Chem. Phys.*, **3**(5), 1769–1778, doi:10.5194/acp-3-1769-2003.
- Engvall, A.-C., R. Krejci, J. Ström, A. Minikin, R. Treffeisen, A. Sthol, and A. Herber (2008a), In-situ airborne observations of the microphysical properties of the Arctic tropospheric aerosol during late spring and summer, *Tellus, Ser. B*, **60**, 392–404.
- Engvall, A.-C., R. Krejci, J. Ström, R. Treffeisen, R. Scheele, O. Hermansen, and J. Paatero (2008b), Changes in aerosol properties during spring-

- summer period in the Arctic troposphere, *Atmos. Chem. Phys.*, **8**, 445–462, doi:10.5194/acp-8-445-2008.
- Flanner, M. G., C. S. Zender, J. T. Randerson, and P. J. Rasch (2007), Present-day climate forcing and response from black carbon in snow, *J. Geophys. Res.*, **112**, D11202, doi:10.1029/2006JD008003.
- Flanner, M. G., C. S. Zender, P. G. Hess, N. M. Mahowald, T. H. Painter, V. Ramanathan, and P. J. Rasch (2009), Springtime warming and reduced snow cover from carbonaceous particles, *Atmos. Chem. Phys.*, **9**(7), 2481–2497, doi:10.5194/acp-9-2481-2009.
- Fuelberg, H. E., D. L. Harrigan, and W. Sessions (2010), A meteorological overview of the ARCTAS 2008 mission, *Atmos. Chem. Phys.*, **10**(2), 817–842, doi:10.5194/acp-10-817-2010.
- Garrett, T. J., and C. Zhao (2006), Increased Arctic cloud longwave emissivity associated with pollution from mid-latitudes, *Nature*, **440**(7085), 787–789, doi:10.1038/nature04636.
- Hansen, J., and L. Nazarenko (2004), Soot climate forcing via snow and ice albedos, *Proc. Natl. Acad. Sci. U. S. A.*, **101**(2), 423–428, doi:10.1073/pnas.2237157100.
- Harrigan, D. L., H. E. Fuelberg, I. J. Simpson, D. R. Blake, G. R. Carmichael, and G. S. Diskin (2011), Transport of anthropogenic emissions during ARCTAS-A: A climatology and regional case studies, *Atmos. Chem. Phys. Discuss.*, **11**, 5435–5491, doi:10.5194/acpd-11-5435-2011.
- Heintzenberg, J., C. Leck, W. Birmili, B. Wehner, M. Tjernström, and A. Wiedensohler (2006), Aerosol number-size distributions during clear and fog periods in the summer high Arctic: 1991, 1996, and 2001, *Tellus, Ser. B*, **58**, 41–50, doi:10.1111/j.1600-0889.2005.00171.x.
- Huang, L., S. L. Gong, C. Q. Jia, and D. Lavoué (2010), Relative contributions of anthropogenic emissions to black carbon aerosol in the Arctic, *J. Geophys. Res.*, **115**, D19208, doi:10.1029/2009JD013592.
- Huffman, G. J., R. F. Adler, M. M. Morrissey, D. T. Bolvin, S. Curtis, R. Joyce, B. McGavock, and J. Susskind (2001), Global precipitation at one-degree daily resolution from multisatellite observations, *J. Hydrometeorol.*, **2**, 36–50, doi:10.1175/1525-7541(2001)002<0036:GPAODD>2.0.CO;2.
- Jacob, D. J., et al. (2010), The Arctic Research of the Composition of the Troposphere from Aircraft and Satellites (ARCTAS) mission: Design, execution, and first results, *Atmos. Chem. Phys.*, **10**(11), 5191–5212, doi:10.5194/acp-10-5191-2010.
- Jiang, H., G. Feingold, W. R. Cotton, and P. G. Duynkerke (2001), Large-eddy simulations of entrainment of cloud condensation nuclei into the Arctic boundary layer: May 18, 1998, FIRE/SHEBA case study, *J. Geophys. Res.*, **106**(D14), 15,113–15,122, doi:10.1029/2000JD900303.
- Klonecki, A., P. Hess, L. Emmons, L. Smith, J. Orlando, and D. Blake (2003), Seasonal changes in the transport of pollutants into the Arctic troposphere-model study, *J. Geophys. Res.*, **108**(D4), 8367, doi:10.1029/2002JD002199.
- Koch, D., et al. (2009), Evaluation of black carbon estimations in global aerosol models, *Atmos. Chem. Phys.*, **9**, 9001–9026, doi:10.5194/acp-9-9001-2009.
- Kondo, Y., L. Sahu, N. Moteki, F. Khan, N. Takegawa, X. Liu, M. Koike, and T. Miyakawa (2010), Consistency and traceability of black carbon measurements made by laser-induced incandescence, thermal-optical transmittance, and filter-based photo-absorption techniques, *Aerosol Sci. Technol.*, **45**, 295–312, doi:10.1080/02786826.2010.533215.
- Kondo, Y., et al. (2011), Emissions of black carbon, organic, and inorganic aerosols from biomass burning in North America and Asia in 2008, *J. Geophys. Res.*, **116**, D08204, doi:10.1029/2010JD015152.
- Law, K. S., and A. M. Stohl (2007), Arctic air pollution: Origins and impacts, *Science*, **315**(5818), 1537–1540, doi:10.1126/science.1137695.
- Leaitch, W. R., R. M. Hoff, and J. I. MacPherson (1989), Airborne and lidar measurements of aerosol and cloud particles in the troposphere over Alert Canada in April 1986, *J. Atmos. Chem.*, **9**, 187–211, doi:10.1007/BF00052832.
- Leaitch, W. R., L. A. Barrie, J. W. Bottenheim, S. M. Li, P. B. Shepson, K. Muthuramu, and Y. Yokouchi (1994), Airborne observations related to ozone depletion at polar sunrise, *J. Geophys. Res.*, **99**(D12), 25,499–25,517, doi:10.1029/94JD02750.
- Leaitch, W. R., et al. (2009), Evidence for Asian dust effects from aerosol plume measurements during INTEX-B 2006 near Whistler, BC, *Atmos. Chem. Phys.*, **9**, 3523–3546, doi:10.5194/acp-9-3523-2009.
- Lubin, D., and A. M. Vogelmann (2006), A climatologically significant aerosol longwave indirect effect in the Arctic, *Nature*, **439**(7075), 453–456, doi:10.1038/nature04449.
- Lubin, D., and A. M. Vogelmann (2010), Observational quantification of a total aerosol indirect effect in the Arctic, *Tellus, Ser. B*, **62**, 181–189, doi:10.1111/j.1600-0889.2010.00460.x.
- Matsui, H., et al. (2011), Seasonal variation of the transport of black carbon aerosol from the Asian continent to the Arctic during the ARCTAS aircraft campaign, *J. Geophys. Res.*, **116**, D05202, doi:10.1029/2010JD015067.
- Mauritsen, T., et al. (2011), An Arctic CCN-limited cloud-aerosol regime, *Atmos. Chem. Phys.*, **11**, 165–173, doi:10.5194/acp-11-165-2011.
- McKendry, I., et al. (2011), Californian forest fire plumes over Southwestern British Columbia: Lidar, sunphotometry, and mountaintop chemistry observations, *Atmos. Chem. Phys.*, **11**, 465–477, doi:10.5194/acp-11-465-2011.
- Moteki, N., and Y. Kondo (2007), Effects of mixing state on black carbon measurements by laser-induced incandescence, *Aerosol Sci. Technol.*, **41**(4), 398–417, doi:10.1080/02786820701199728.
- Moteki, N., and Y. Kondo (2010), Dependence of laser-induced incandescence on physical properties of black carbon aerosols: Measurements and theoretical interpretation, *Aerosol Sci. Technol.*, **44**(8), 663–675, doi:10.1080/02786826.2010.484450.
- Oshima, N., et al. (2004), Asian chemical outflow to the Pacific in late spring observed during the PEACE-B aircraft mission, *J. Geophys. Res.*, **109**, D23S05, doi:10.1029/2004JD004976.
- Petters, M. D., and S. M. Kreidenweis (2007), A single parameter representation of hygroscopic growth and cloud condensation nucleus activity, *Atmos. Chem. Phys.*, **7**, 1961–1971, doi:10.5194/acp-7-1961-2007.
- Quinn, P. K., T. L. Miller, T. S. Bates, J. A. Ogren, E. Andrews, and G. E. Shaw (2002), A 3-year record of simultaneously measured aerosol chemical and optical properties at Barrow, Alaska, *J. Geophys. Res.*, **107**(D11), 4130, doi:10.1029/2001JD001248.
- Radke, L. F., J. H. Lyons, D. A. Hegg, and P. V. Hobbs (1984), Airborne observations of Arctic aerosols. I: Characteristics of Arctic haze, *Geophys. Res. Lett.*, **11**, 393–396, doi:10.1029/GL011i005p00393.
- Sachse, G. W., G. F. Hill, L. O. Wade, and M. G. Perry (1987), Fast-response, high precision carbon monoxide sensor using a tunable diode laser absorption technique, *J. Geophys. Res.*, **92**, 2071–2081, doi:10.1029/JD092iD02p02071.
- Schnell, R. C., and W. E. Raatz (1984), Vertical and horizontal characteristics of Arctic haze during AGASP: Alaskan Arctic, *Geophys. Res. Lett.*, **11**, 369–372, doi:10.1029/GL011i005p00369.
- Sessions, W. R., H. F. Fuelberg, R. A. Kahn, and M. G. Winker (2010), An investigation of methods for injecting emissions from boreal wildfires using WRF-Chem during ARCTAS, *Atmos. Chem. Phys. Discuss.*, **10**, 26,551–26,606, doi:10.5194/acpd-10-26551-2010.
- Shaw, G. E. (1995), The Arctic haze phenomenon, *Bull. Am. Meteorol. Soc.*, **76**(12), 2403–2413, doi:10.1175/1520-0477(1995)076<2403:TAHP>2.0.CO;2.
- Shindell, D., and G. Faluvegi (2009), Climate response to regional radiative forcing during the twentieth century, *Nat. Geosci.*, **2**(4), 294–300, doi:10.1038/ngeo473.
- Shindell, D. T., et al. (2008), A multi-model assessment of pollution transport to the Arctic, *Atmos. Chem. Phys.*, **8**(17), 5353–5372, doi:10.5194/acp-8-5353-2008.
- Staebler, R. M., G. den Hartog, B. Georgi, and T. Dürsterdiek (1994), Aerosol size distributions in Arctic haze during the Polar Sunrise Experiment 1992, *J. Geophys. Res.*, **99**, 25,429–25,437, doi:10.1029/94JD00520.
- Staebler, R. M., D. Toom-Sauntry, L. Barrie, U. Langendörfer, E. Lehner, S.-M. Li, and H. Dryfhout-Clark (1999), Physical and chemical characteristics of aerosols at Spitsbergen in the spring of 1996, *J. Geophys. Res.*, **104**(D5), 5515–5529, doi:10.1029/1998JD100056.
- Stocks, B. J., et al. (1998), Climate change and forest fire potential in Russian and Canadian boreal forests, *Clim. Change*, **38**(1), 1–13, doi:10.1023/A:1005306001055.
- Stohl, A. (2001), A 1-year Lagrangian “climatology” of airstreams in the Northern Hemisphere troposphere and lowermost stratosphere, *J. Geophys. Res.*, **106**(D7), 7263–7279, doi:10.1029/2000JD900570.
- Stohl, A. (2006), Characteristics of atmospheric transport into the Arctic troposphere, *J. Geophys. Res.*, **111**, D11306, doi:10.1029/2005JD006888.
- Streets, D. G., et al. (2003), An inventory of gaseous and primary aerosol emissions in Asia in the year 2000, *J. Geophys. Res.*, **108**(D21), 8809, doi:10.1029/2002JD003093.
- Ström, J., J. Umegård, K. Tørseth, P. Tunved, H.-C. Hansson, K. Holmén, V. Wismann, A. Herver, and G. König-Langlo (2003), One year of particle size distribution and aerosol chemical composition measurements at the Zeppelin station, Svalbard, March 2000–2001, *Phys. Chem. Earth*, **28**, 1181–1190.
- Warneke, C., et al. (2006), Biomass burning and anthropogenic sources of CO over New England in the summer 2004, *J. Geophys. Res.*, **111**, D23S15, doi:10.1029/2005JD006878.
- Warneke, C., et al. (2009), Biomass burning in Siberia and Kazakhstan as an important source for haze over the Alaskan Arctic in April 2008, *Geophys. Res. Lett.*, **36**, L02813, doi:10.1029/2008GL036194.
- Warneke, C., et al. (2010), An important contribution to springtime Arctic aerosol from biomass burning in Russia, *Geophys. Res. Lett.*, **37**, L01801, doi:10.1029/2009GL041816.

- Weber, R. J., et al. (2003), New particle formation in anthropogenic plumes advecting from Asia observed during TRACE-P, *J. Geophys. Res.*, *108*(D21), 8814, doi:10.1029/2002JD003112.
- Wisthaler, A., A. Hansel, R. R. Dickerson, and P. J. Crutzen (2002), Organic trace gas measurements by PTR-MS during INDOEX 1999, *J. Geophys. Res.*, *107*(D19), 8024, doi:10.1029/2001JD000576.
- Yamanouchi, T., et al. (2005), Arctic Study of Tropospheric Aerosol and Radiation (ASTAR) 2000: Arctic haze case study, *Tellus, Ser. B*, *57*(2), 141–152, doi:10.1111/j.1600-0889.2005.00140.x.
- Yum, S. S., and J. G. Hudson (2001), Vertical distributions of cloud condensation nuclei spectra over the springtime Arctic Ocean, *J. Geophys. Res.*, *106*(D14), 15,045–15,052, doi:10.1029/2000JD900357.
- Zhang, Q., et al. (2009), Asian emissions in 2006 for the NASA INTEX-B mission, *Atmos. Chem. Phys.*, *9*, 5131–5153, doi:10.5194/acp-9-5131-2009.
- B. E. Anderson and G. Diskin, Chemistry and Dynamics Branch, NASA Langley Research Center, MS 483, Hampton, VA 23681-2199, USA.
- D. R. Blake, Department of Chemistry, University of California, Irvine, 570 Rowland Hall, Irvine, CA 92697-2025, USA.
- M. J. Cubison and J. L. Jimenez, CIRES, University of Colorado at Boulder, UCB 216, Boulder, CO 80309, USA.
- H. E. Fuelberg and W. R. Sessions, Department of Meteorology, Florida State University, 404 Love Bldg., MC 4520, Tallahassee, FL 32306-4520, USA.
- M. Koike, Y. Kondo, H. Matsui, and N. Moteki, Department of Earth and Planetary Science, Graduate School of Science, University of Tokyo, Hongo 7-3-1 Bunkyo-ku, Tokyo 113-0033, Japan. (matsui@eps.s.u-tokyo.ac.jp)
- L. K. Sahu, Department of Space, Physical Research Laboratory, Ahmedabad 380009, India.
- N. Takegawa, Research Center for Advanced Science and Technology, University of Tokyo, 4-6-1 Komaba Meguro-ku, Tokyo 153-8904, Japan.
- A. Wisthaler, Institute of Ion Physics and Applied Physics, University of Innsbruck, Technikerstrasse 25, A-6020 Innsbruck, Austria.
- Y. Zhao, Air Quality Research Center, University of California, Davis, 2132 Bainer Hall, One Shields Ave., Davis, CA 95616, USA.